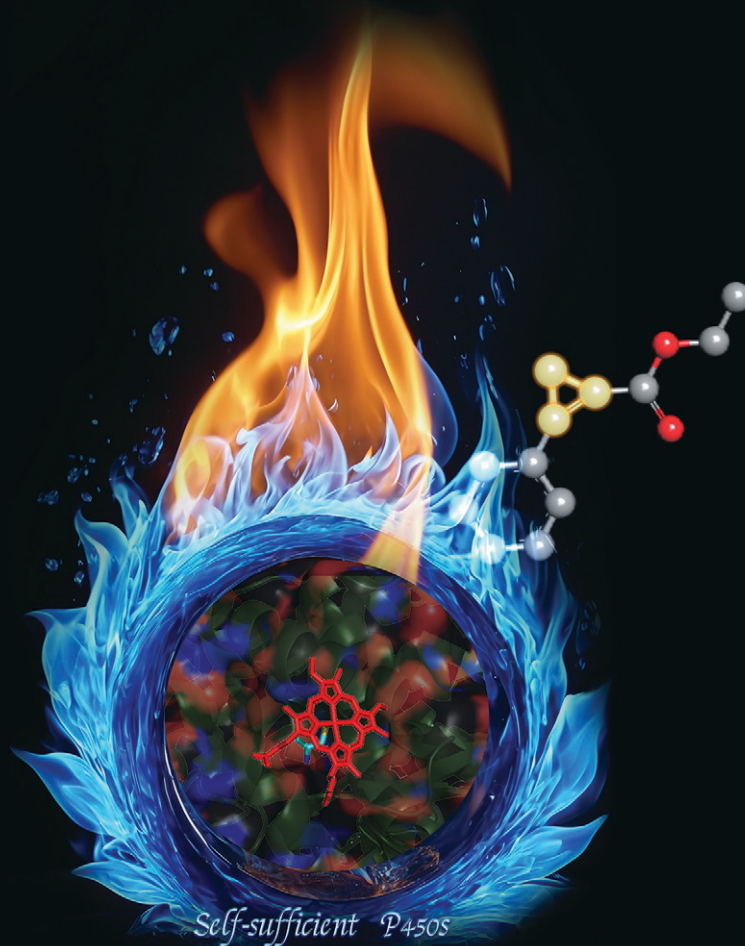


Catalysis Science & Technology

Volume 14
Number 4
21 February 2024
Pages 779-1074

rsc.li/catalysis



ISSN 2044-4761

COMMUNICATION

Guochao Xu, Ye Ni *et al.*
Modulating stereoselectivity and catalytic efficiency of
carbenoid reactions catalysed by self-sufficient P450s

Cite this: *Catal. Sci. Technol.*, 2024, 14, 835Received 10th September 2023,
Accepted 29th November 2023

DOI: 10.1039/d3cy01258a

rsc.li/catalysis

Self-sufficient P450s are versatile biocatalysts. Among six self-sufficient P450 backbones, two variants from *Tepidiphilus thermophilus* exhibited a high TOF value of 1.5 min^{-1} (P450_{TT-C385S}) and excellent diastereoselectivity of $d_e = 95.4\%$ (P450_{TT-C385H}). Molecular simulation was performed to reveal the different catalytic mechanisms among the self-sufficient P450 backbones. This work could provide useful information for exploring challenging unnatural reactions.

Carbenoid reactions, as powerful reactions, can effectively construct fundamental building blocks of organic molecules, including C–C, C–Si, C–N bonds, *etc.*¹ They could be used to construct complex organic molecules, introduce functional groups, achieve reaction selectivity, and exhibit reaction diversity. Thereby they provide possibilities to expand the catalytic capabilities of nature for a sustainable chemical industry.² Traditional carbene reactions are derived from transition metal-catalyzed reactions (such as Rh, Ru, Pd, Co, Fe). In 2012, Arnold *et al.* discovered that heme containing proteins could catalyse styrene cyclopropanation when a diazo carbene precursor is provided (Fig. 1a). This enzymatic catalysis of carbene reactions was previously unknown.³ The biocatalytic carbene transfer reactions demonstrated by these heme containing proteins are often complementary to the state-of-the-art processes based on small-molecule transition-metal catalysts.³ This highlights that engineered biocatalysts are valuable addition to the toolbox of synthetic chemists.³ Moreover, with asymmetric three-dimensional structures, heme containing proteins can provide precise chiral synthesis while creating unnatural enzymatic reactions. The biocatalytic platform offers an exciting opportunity to tackle challenging problems in modern synthetic chemistry and selective catalysis.⁴

Key Laboratory of Industrial Biotechnology, Ministry of Education, School of Biotechnology, Jiangnan University, Wuxi 214122, Jiangsu, China.

E-mail: guochaoxu@jiangnan.edu.cn, yni@jiangnan.edu.cn

† Electronic supplementary information (ESI) available. See DOI: <https://doi.org/10.1039/d3cy01258a>

Modulating stereoselectivity and catalytic efficiency of carbenoid reactions catalysed by self-sufficient P450s†

Binhao Wang, Cuiping You, Guochao Xu * and Ye Ni *

P450 monooxygenases are important biocatalysts possessing vital functions,⁵ most typically represented by their ability to catalyse a series of challenging reactions. Active iron-oxo intermediate compound I is required for the oxidative activity of P450s, strikingly similar to the carbenoid active intermediate.⁶ P450s gain electrons from NAD(P)H and delocalize N_2 as a leaving group to generate carbene-reactive intermediates and thus catalyse the generation of carbenes (Fig. 1b).⁷ In addition, a series of heme proteins such as myoglobin, lactococcal multidrug resistance regulator and cytochrome C have also been shown to catalyse carbenoid reactions (Fig. 1c–e).⁸ Compared with other heme proteins, self-sufficient P450s allow efficient electron transfer through a polypeptide chain linking the heme domain and redox partner (*e.g.*, flavoenzymes and iron-sulfur). There is no need to search for suitable redox partners to establish a functional system. Moreover, the reductase domain can furnish electrons to other enzymes in chimeric fusion proteins, while the P450 domain can be engineered for high activity and

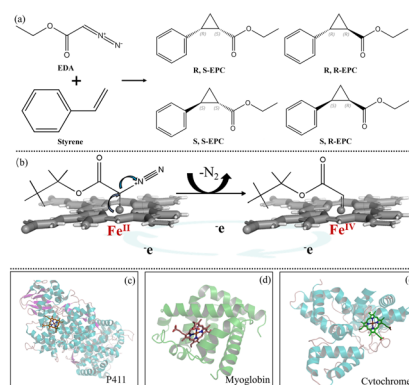


Fig. 1 Carbene reaction and the protein structures of three reported enzyme backbones with excellent performance in carbene reactions. (a) Styrene cyclopropanation as the carbenoid model reaction. (b) Formation of active intermediates in the carbene reaction. (c) P411 (PDB: 4H23). (d) Myoglobin (PDB: 1A6K). (e) Cytochrome C (PDB: 1YNR).

selectivity.⁹ Some of them, derived from extreme environments, also exhibit stability even under harsh conditions.¹⁰ Introducing artificial enzymes of transition metals is expensive and of low economic value compared with heme containing enzymes, which depend on cheap metallic iron. Therefore, exploring efficient self-sufficient P450 backbones with high enantioselectivity for synthesizing carbene stereoisomers is of great importance for discovering challenging unnatural reactions, and also could provide guidance to engineering existing P450s to extend their boundaries for natural reactions. Herein, six self-sufficient P450s were evaluated using the carbenoid model reaction of cyclopropanation of ethyl diazoacetate (EDA) (Fig. 1a). The molecular basis of carbenoid reactions catalysed by different self-sufficient P450 backbones was investigated.

Here, using three well studied enzymes with excellent catalytic performance in carbenoid reactions as probes (P411-CIS derived from *Priestia megaterium*,¹¹ myoglobin derived from *Physeter catodon*¹² and cytochrome C derived from *Rhodothermus marinus*¹³), genome mining was performed. Six P450s derived from *Tepidiphilus thermophilus* (P450_{TT} also known as CYP116B46 (ref. 14)), *Jhaorihella thermophiles* (P450_{JT} also known as CYP116B63 (ref. 14)), *Aspergillus fumigatus* (CYP505X identified by R. Weis *et al.*¹⁵), *Myceliophthora thermophila* (CYP505A30 identified by G. J. Baker *et al.*¹⁶), *Bacillus methanolicus* (CYP152K6 identified by Hazel M. Girvan *et al.*¹⁷), and *Collariella virescens* (CviUPO also known as rCviUPO¹⁸) were chosen as candidate enzymes. The phylogenetic tree was employed to analyse the relationship between P450_{BM3}, myoglobin (also with activity in the carbene reaction) and six self-sufficient P450s. Among them, CviUPO is the most closely related to myoglobin. CYP505X originates from a common ancestral branch with P450_{BM3}. Similarly, P450_{TT} and P450_{JT} are derived from an ancestral branch with myoglobin, specifically, they belong to two different subfamilies. P450_{JT} was observed to exhibit better catalytic activity than P450_{TT} (Fig. 2a), reflecting the functional differences that arose from the specific differentiation of CYP116 during evolution. Among them, CYP152K6 has the furthest relationship with others. P450s have several highly conserved regions which could be associated with their secondary structures.¹⁹ As expected, despite low degrees of sequence identity, the different P450s share a few conserved key catalytic residues and a common fold (Fig. 2b). The conservative domains (90–290 amino acids) of the six P450s are highly similar. Composed of a hydrophobic amino acid, they can enhance the stability of the inner core (Fig. 2b). The conserved catalytic domain sequences of the six P450s provide possibilities to catalyse carbenoid reactions. The performance of the six P450s was evaluated in carbenoid model reactions.

The cyclopropanation activity of P450s is highly dependent on the electronic properties of the proximal ligand.^{8,20} To increase the redox potential for reducing the resting Fe^{III}-heme to Fe^{II}-heme, the vigorous electron donor cystine at the axial ligand of the heme cofactor was substituted with a

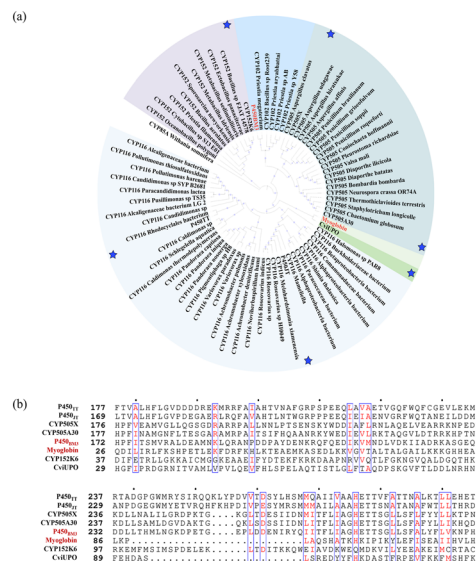


Fig. 2 Phylogenetic tree and sequence alignment for P450_{BM3}, myoglobin and six self-sufficient P450s. (a) Phylogenetic tree. Blue stars: six self-sufficient P450s. (b) Sequence alignment. The alignment shows the implicitly conserved catalytic domain (blue box).

weaker electron donor serine or histidine. Herein, the six self-sufficient P450s were evaluated with the carbenoid model reaction of styrene and EDA as substrates. Under assay conditions, crude enzymes of the six P450 backbones could catalyse the carbenoid model reaction (Fig. S7–S13[†]). Based on the carbenoid reaction performances of the different self-sufficient P450 crude enzymes (Fig. S7–S13[†]), enzymes with high TOF potential (according to detection responses) and excellent stereoselectivity were purified for further research. Initially, the turnover frequencies of the model carbenoid reaction among seven candidates were compared using purified P450s. Furthermore, P411/P450-CIS¹¹ and two other backbones (myoglobin¹² and cytochrome C¹³) were chosen as positive controls (Fig. 3), which have been reported with high turnover frequencies and stereoselectivity in carbenoid reactions. Under assay conditions, the TOF ratio of P411-CIS and P450-CIS was approximately 1:1.3, consistent with their reported conversion rate ratio,¹¹ and was higher than that of the cytochrome C backbone. However, the turnover frequencies of the two enzymes were lower than that of the myoglobin backbone. Notably, under the same conditions, the seven tested self-sufficient P450s had higher conversion rates than all four positive controls. Among all the tested purified enzymes, P450_{TT}-C385S showed the highest TOF (1.5 min⁻¹), which is 4.3 times higher than that of P411-CIS (0.35 min⁻¹), and 3 times higher than that of P450_{JT}-WT with the 2nd highest TOF value (1.2 min⁻¹). It is worth noting that both P450_{TT}-C385S and P450_{JT}-C377S displayed higher TOF than that substituted with His. CYP505X-WT displayed a moderate TOF value (0.95 min⁻¹) compared with P450_{JT}-WT and P450_{TT}-C385S. All the TOF values of purified P450s were consistent with their UV response in crude enzyme reactions (Fig. S7[†]).

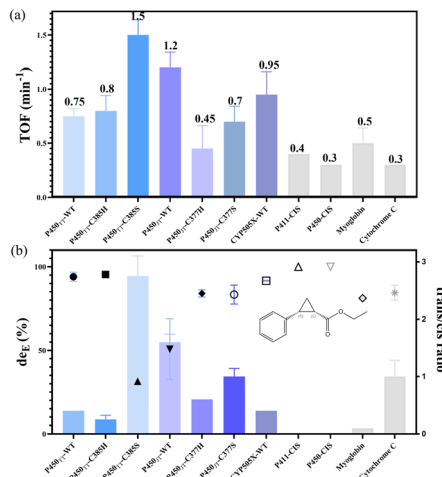


Fig. 3 Comparison of turnover frequencies (TOFs) and stereoselectivity of the carbenoid model reaction catalysed by different purified P450s. (a) Turnover frequencies. (b) Diastereoselectivity and *trans/cis* ratio. Dots: diastereoselectivity. Columns: *trans/cis* ratio. Reactions were performed with 10 μ M enzyme, 10 mM styrene, 20 mM EDA, and 10 mM Na₂S₂O₄ in 100 mM Tris-HCl (pH = 8.0). Stereoselectivity was determined by ultra-performance convergence chromatography

$$\frac{trans}{cis} \text{ ratio} = \frac{SS + RR}{SR + RS} \quad de_E = \frac{RR + RS - SR - SS}{SS + SR + RS + RR}$$

Some proteins in *E. coli* exhibit significant background in crude enzyme reactions, particularly for poorly expressed or unstable P450s.²¹ As carbene transfer biocatalysts, the stereoselectivity is regarded as a critical character. Under assay conditions, purified P450-CIS displayed excellent diastereoselectivity as P411-CIS (99.9%), dominated by *R,S*-ethyl 2-phenylcyclopropane carboxylate (*R,S*-EPC) (Table S4[†]). Among all the tested purified enzymes, almost perfect diastereoselectivity was observed with P450_{JT}-C385H (95.4%), P450_{JT}-WT (94.0%), and CYP505X-WT (91.6%). Slightly inferior to the above three enzymes, P450_{JT}-C377H (84.0%) and P450_{JT}-C377S (83.3%) showed impressive diastereoselectivity performance (Table S4[†]). P450_{JT}-WT (50.7%) and P450_{JT}-C385S (31.5%) displayed relatively poor diastereoselectivity. An almost excellent *trans/cis* ratio was also observed in P450_{JT}-C385H (0.2), which was slightly inferior than that of P411-CIS (0) and P450-CIS (0) (Fig. 3b). Notably, all the enzymes produced a *cis*-stereoisomer relatively rich in (*R,S*)-EPC, while the *trans*-stereoisomer was rich in (*R,R*)-EPC. Among them, P450_{JT}-WT, P450_{JT}-C385H, P450_{JT}-C377H, and CYP505X-WT all displayed excellent *cis*-selectivity ($ee_{cis} = 99.9\%$) while maintaining high de_E values. Differently, P450_{JT}-C377S had a moderate enantioselectivity ($de_E = 83.3\%$, $ee_{cis} = 93.5\%$, $ee_{trans} = 51.9\%$) (Fig. 3b, Table S4[†]). Although the myoglobin backbone had a higher turnover frequency than P411-CIS, the diastereoselectivity of myoglobin (81.1%) was inferior to that of P411-CIS (99.9%) and the other self-sufficient P450s (P450_{JT}-WT, P450_{JT}-C285H, CYP505X-WT) tested (Fig. 3b). Compared with the tested P450s, cytochrome C displayed only moderate turnover frequency (0.30 min⁻¹) and

diastereoselectivity ($de_E = 84.4\%$). It is speculated that the complete electron transport chain of self-sufficient P450s could provide more vigorous catalytic power to allow higher turnover frequencies.

With the determined and refined crystal structure, P450_{BM3} and P450_{JT} could be used as excellent model proteins to investigate the influence of intramolecular electron transport chains in the carbenoid model reaction. The edge-to-edge straight-line distances of FMN-heme (P450_{BM3}) and [2Fe-2S]-heme (P450_{JT}) are 18.6 Å and 25.3 Å, respectively.²² Several residues between [2Fe-2S] and heme of P450_{JT} may contribute to the electron delivery path (Fig. 4a).²² These residues predominantly consist of acidic residues (E723, E729) and basic residues (R388, R718). Notably, a pattern of alternating positively charged (arginine) and negatively charged (glutamine) amino acids was observed in adjacent positions. These residues play a crucial role in facilitating smooth electron transfer by providing redox potentials along their main chains. Furthermore, it was observed that certain polar residues (C385, Q725, S726), which lack aromatic groups, exhibited unexpectedly low dependence on distance.²¹ This phenomenon can be attributed to the specific configurations of their side chains.²¹ In P450_{JT}, the efficient peptide electron transfer chains might play a more important role than the “domain close” interaction observed in P411-CIS, which relies on FMN-heme domain interaction. Consequently, a higher catalytic activity (TOF) was observed with P450_{JT} (Fig. 4a).

The interactions of heme-iron and nearby residues were analysed (Fig. S14a-f[†]). It was found that a cluster of hydrophobic residues is located near the heme-iron, facilitating strong hydrophobic interactions at the core. These residues collectively create a compact hydrophobic pocket that allows the insertion of the heme cofactor in the interior of the pocket.²³ Moreover, multiple nonpolar and aromatic residues were also observed in the active site and substrate

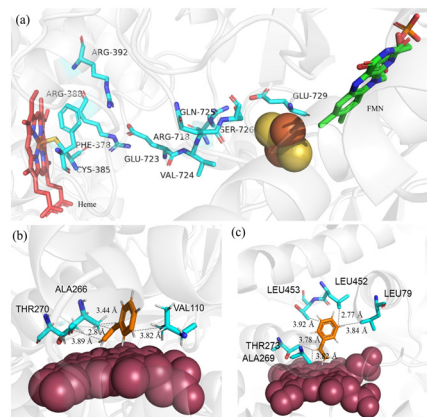


Fig. 4 Molecular mechanism analysis. (a) Residues proposed by Guo *et al.* that may have contributed to long-range electron transfer between [2Fe-2S] and heme of P450_{JT} (PDB ID: 2HPD). Molecular docking of substrate styrene with (b) P450_{JT} and (c) CYP505X. Red sphere: heme cofactor. Blue sticks: residues interacting with substrates. Black dashed lines: interaction distances.

channel. These residues have been proved to dominate the cone-shaped active site and help P450s accept hydrophobic substrates (Fig. S14a–f†).^{24,25} For CviUPO, the substrate binds heme with high affinity in a hydrophobic pocket, which is composed of eighteen nonpolar residues, including P21 (3.98 Å), A22 (3.17 Å), L48 (3.26 Å) and F52 (2.98 Å). In addition to the salt bridge between R97 (5.08 Å) and the carbonyl group that stabilizes the porphyrin conformation (also observed in most members of the CYP116 subfamily²⁶), a number of residues were observed to engage in hydrogen bonds with heme, including E90 (2.56 Å), H91 (1.85 Å), L95 (1.63 Å), S96 (2.30 Å) and R97 (3.34 Å). Additionally, H91 may also coordinate with heme through an imidazole moiety.²⁶ All these interactions provide CviUPO with excellent catalytic performance in the carbenoid model reaction, despite the low soluble protein expression observed (Fig. S2†).

P450_{JT} exhibited relatively poor diastereoselectivity compared with CYP505X. To understand the mechanisms of stereoselectivity in the carbenoid model reaction, molecular simulation of CYP505X ($de_E = 91.6\%$) and P450_{JT} ($de_E = 50.7\%$) complexes was conducted (Fig. 4b and c). For P450_{JT}, hydrophobic interactions with the substrate were generated by three nonpolar residues (V110, A266, T270). All the interactions between the substrate and surrounding residues were observed to occur within a distance range of 2.8–3.9 Å. In addition, all of them were observed in an unbalanced manner around styrene (only one force acting on the benzene ring portion, while the rest were distributed on the same side of the substrate) (Fig. 4b). Unbalanced forces with the hydrophobic substrate resulted in a “tilted” conformation in P450_{JT} (Fig. 4b). By contrast, a more “vertical” conformation was observed in CYP505X, benefiting from more uniform forces with the substrate (Fig. 4c). All the hydrophobic interactions with the substrate are formed with five residues (L79, A269, T273, L452 and T453). Five forces were evenly distributed in the benzene ring and olefin, resulting in a relatively “vertical” form where the substrate could “stand” on the porphyrin. The morphology of the substrate binding to the active site of enzymes leads to the difference in stereoselectivity of the final product. Enhanced *cis*-selectivity could be obtained when the terminal olefin of the substrate approaches the porphyrin at a perpendicular angle in the carbenoid model reaction, consistent with those reported by others.²⁷

Conclusions

In conclusion, excellent potential carbenoid reaction backbones (CYP505X) and mutants with high TOF (P450_{TT}-C385S) and excellent stereoselectivity (P450_{TT}-C385H) were obtained based on their catalytic performances. The study of electron transfer pathways between P450_{TT} and P450_{BM3} revealed that more efficient electron transfer can lead to increased catalytic activity in the carbenoid model reaction. In addition, the influence of the heme axial key residue and hydrophobic environment of the heme pocket on the

carbenoid model reaction was also investigated. Substituting the crucial axial residue with a weaker electron donor enhanced the catalytic activities in carbenoid model reactions for most P450s. However, in the case of P450_{JT}, P450_{JT}-WT exhibited higher catalytic activity (TOF) than variants P450_{JT}-C377H and P450_{JT}-C377S. For CviUPO, although poor protein expression was observed, the strong hydrophobic interaction in the core region contributes to its surprising catalytic performance. Based on molecular simulation analysis of P450_{JT} and CYP505X complexes with the substrate, a perpendicular conformation of the terminal olefin of the substrate in the porphyrin is conducive to better *cis*-selectivity in carbenoid model reactions. This work provides promising self-sufficient P450s for carbenoid reactions and instructive information for exploring the application of enzymatic carbenoid reactions.

Author contributions

B. W., G. X. and Y. N. conceived and designed the project. B. W. conducted enzyme screening, characterization and mutation. C. Y. performed stereoselectivity analysis. B. W. carried out the computation analysis. B. W., G. X. and Y. N. wrote the manuscript. G. X. and Y. N. obtained financial support for the project leading to this publication.

Conflicts of interest

There are no conflicts to declare.

Acknowledgements

We are grateful to the National Key R&D Program (2021YFC2102700) and the National Natural Science Foundation of China (22078127, 22077054) for the financial support.

Notes and references

- 1 F. H. Arnold, *Q. Rev. Biophys.*, 2015, **48**, 404–410.
- 2 F. H. Arnold, *Angew. Chem., Int. Ed.*, 2018, **57**, 4143–4148.
- 3 Z. Liu and F. H. Arnold, *Curr. Opin. Biotechnol.*, 2021, **69**, 43–51.
- 4 Y. Yang and F. H. Arnold, *Acc. Chem. Res.*, 2021, **54**, 1209–1225.
- 5 V. B. Urlacher and M. Girhard, *Trends Biotechnol.*, 2019, **37**, 882–897.
- 6 T. K. Hyster and F. H. Arnold, *Isr. J. Chem.*, 2015, **55**, 14–20.
- 7 P. C. E. Moody and E. L. Raven, *Acc. Chem. Res.*, 2018, **51**, 427–435.
- 8 P. Srivastava, H. Yang, K. Ellis-Guardiola and J. C. Lewis, *Nat. Commun.*, 2015, **6**, 7789.
- 9 L. L. Zhang, Z. Z. Xie, Z. W. Liu, S. Y. Zhou, L. X. Ma, W. D. Liu, J. W. Huang, T. P. Ko, X. Q. Li, Y. C. Hu, J. Min, X. J. Yu, R. T. Guo and C. C. Chen, *Nat. Commun.*, 2020, **11**, 2676.
- 10 D. Correddu, G. Di Nardo and G. Gilardi, *Trends Biotechnol.*, 2021, **39**, 1184–1207.

- 11 Z. J. Wang, H. Renata, N. E. Peck, C. C. Farwell, P. S. Coelho and F. H. Arnold, *Angew. Chem., Int. Ed.*, 2014, **53**, 6810–6813.
- 12 M. Bordeaux, V. Tyagi and R. Fasan, *Angew. Chem., Int. Ed.*, 2015, **54**, 1744–1748.
- 13 S. B. J. Kan, X. Huang, Y. Gumulya, K. Chen and F. H. Arnold, *Nature*, 2017, **552**, 132–136.
- 14 M. Tavanti, J. L. Porter, S. Sabatini, N. J. Turner and S. L. Flitsch, *ChemCatChem*, 2018, **10**, 1042–1051.
- 15 R. Weis, M. Winkler, M. Schittmayer, S. Kambourakis, M. Vink, J. D. Rozzell and A. Glieder, *Adv. Synth. Catal.*, 2009, **351**, 2140–2146.
- 16 G. J. Baker, H. M. Girvan, S. Matthews, K. J. McLean, M. Golovanova, T. N. Waltham, S. E. J. Rigby, D. R. Nelson, R. T. Blankley and A. W. Munro, *ACS Omega*, 2017, **2**, 4705–4724.
- 17 H. M. Girvan, H. Poddar, K. J. McLean, D. R. Nelson, K. A. Hollywood, C. W. Levy, D. Leys and A. W. Munro, *J. Inorg. Biochem.*, 2018, **188**, 18–28.
- 18 D. Linde, E. Santillana, E. Fernández-Fueyo, A. González-Benjumea, J. Carro, A. Gutiérrez, A. T. Martínez and A. Romero, *Antioxidants*, 2022, **11**, 891.
- 19 I. Matsunaga, A. Ueda, N. Fujiwara, T. Sumimoto and K. Ichihara, *Lipids*, 1999, **34**, 841–846.
- 20 J. A. Mcintosh, T. Heel, A. R. Buller, L. Chio and F. H. Arnold, *J. Am. Chem. Soc.*, 2015, **137**, 13861–13865.
- 21 F. Polo, S. Antonello, F. Formaggio, C. Toniolo and F. Maran, *J. Am. Chem. Soc.*, 2005, **127**, 492–493.
- 22 L. Zhang, Z. Xie, Z. Liu, S. Zhou, L. Ma, W. Liu, J. W. Huang, T. P. Ko, X. Li, Y. Hu, J. Min, X. Yu, R. T. Guo and C. C. Chen, *Nat. Commun.*, 2020, **11**, 2676.
- 23 C. Y. Li, G. Anuraga, C. P. Chang, T. Y. Weng, H. P. Hsu, H. D. K. Ta, P. F. Su, P. H. Chiu, S. J. Yang, F. W. Chen, P. H. Ye, C. Y. Wang and M. D. Lai, *J. Exp. Clin. Cancer Res.*, 2023, **42**, 22.
- 24 M. Tavanti, J. L. Porter, C. W. Levy, J. R. G. Castellanos, S. L. Flitsch and N. J. Turner, *Biochem. Biophys. Res. Commun.*, 2018, **501**, 846–850.
- 25 J. C. Aschenbrenner, A. C. Ebrecht, C. Tolmie, M. S. Smit and D. J. Opperman, *Catal. Sci. Technol.*, 2021, **11**, 7359–7367.
- 26 A. Ciaramella, G. Catucci, G. Gilardi and G. Di Nardo, *Int. J. Biol. Macromol.*, 2019, **140**, 577–587.
- 27 S. J. Thompson, M. R. Brennan, S. Y. Lee and G. Dong, *Chem. Soc. Rev.*, 2018, **47**, 929–981.